

## **Research on welding thermal simulation behavior of V-N-Ti and V-Nb-Ti microalloyed steels**

\*Hao Yu<sup>1)</sup> and Bing Yang<sup>2)</sup>

<sup>1), 2)</sup> School of Materials Science and Engineering, University of Science and Technology  
Beijing, Beijing 100083, China  
<sup>1)</sup> [yhzhmr@sina.com](mailto:yhzhmr@sina.com)

### **ABSTRACT**

In this experiment, Specimens of V-N-Ti and V-Nb-Ti steels were heated up to 1350 °C by DIL805A type of thermal expansion, then keep them for 1 s, then cooled down to Ac<sub>3</sub> temperature (870 °C) by the cooling rate of 20 °C /s, and then cooled down to room temperature at different cooling rates of 0.5, 1, 3, 6, 10, 15, 20, 30, 40 and 60 °C/s, respectively. Comparison with the results of the experiment, When the cooling rate is below 6 °C/s, the microstructure of the two kinds of steels is composed of ferrite and pearlite, as the cooling rate is more than 10 °C/s, bainite appeared firstly in the V-Nb-Ti steel; While until the cooling rate is more than 40 °C/s, microstructure of the V-N-Ti steel is almost bainite. Thus, the transformation cooling rate for bainite of the V-Nb-Ti steel rate is lower than that of the V-N-Ti steel.

**Keywords:** welding thermal simulation; welding heat affected zone; nitrogen; microstructure

### **1. INTRODUCTION**

With the development of science and technology, the welding process and the research on the welding materials have got great innovation and progress<sup>[1,2]</sup>. Whether the new type of metal materials and welding joints of welding components can work in heat and stress normally or not are problems which are concerned by the design, manufacture and using department. Therefore, it needs thermal simulation or stress simulation test for welding structure or joint through the simple test methods which provide the necessary technical data and the judgment for the actual project<sup>[3,4]</sup>. And the part near the fusion line in the welding heat affected zone is the weak area of the whole welding joint, which has a direct impact on the whole performance of welding joints, so research on the microstructure evolution of this area during the process of welding is very important in making a reasonable welding process<sup>[5]</sup>.

---

<sup>1)</sup> Professor

<sup>2)</sup> Mr.

## 2. EXPERIMENTAL

The size of samples for the welding thermal simulation is  $\Phi 4 \times 10$  mm. The simulation process curve was made according to the actual welding process of the thermal cycling curve. The reheating rate for welding simulation is fast, and the heating time from room temperature to the highest temperature ( $T_{max}$ ) is 5 ~ 6 s generally, the highest heating temperature is 1300 ~ 1350 °C. The heating rate during the thermal simulation process will be set at 270 °C/s, then heated to the highest temperature of 1350 °C and keep it for 1 s, and then cooled down to  $A_{c3}$  temperature (870 °C) by the cooling rate of 20 °C/s, after this then cooled down to room temperature at different cooling rates of 0.5, 1, 3, 6, 10, 15, 20, 30, 40 and 60 °C/s, respectively. The welding simulation process is shown in Figure 1. This experiment is completed by the DIL805A type of thermal expansion in the efficient rolling national engineering research center in USTB. Different cooling rates of the corresponding  $t_{8/5}$  are listed in Table 2.

Table 1 Chemical compositions of steels, [wt. %]

Steel	C	Si	Mn	P	S	Als	V	Ti	Nb	N
V-N-Ti	0.08	0.18	1.4	0.009	0.0018	0.018	0.066	0.014	--	0.016
V-Nb-Ti	0.08	0.2	1.45	0.007	0.0015	0.023	0.047	0.001	0.028	0.0055

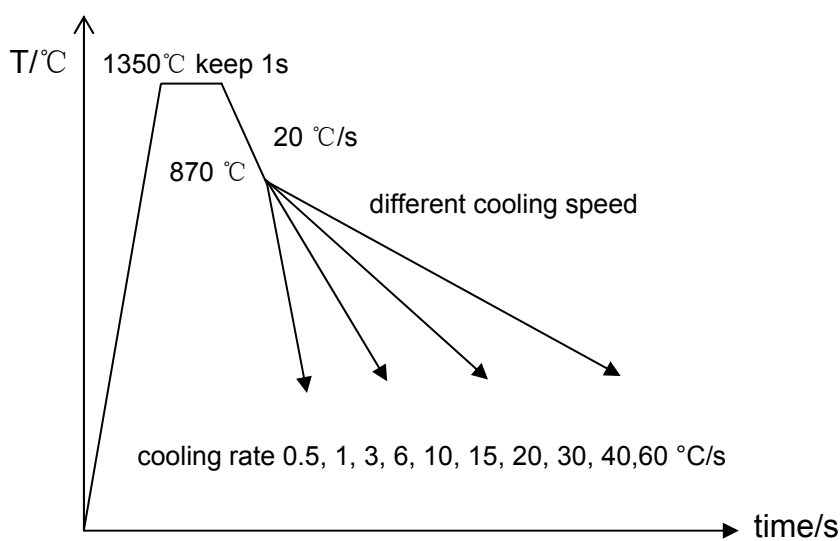


Fig.1 SHCCT process line

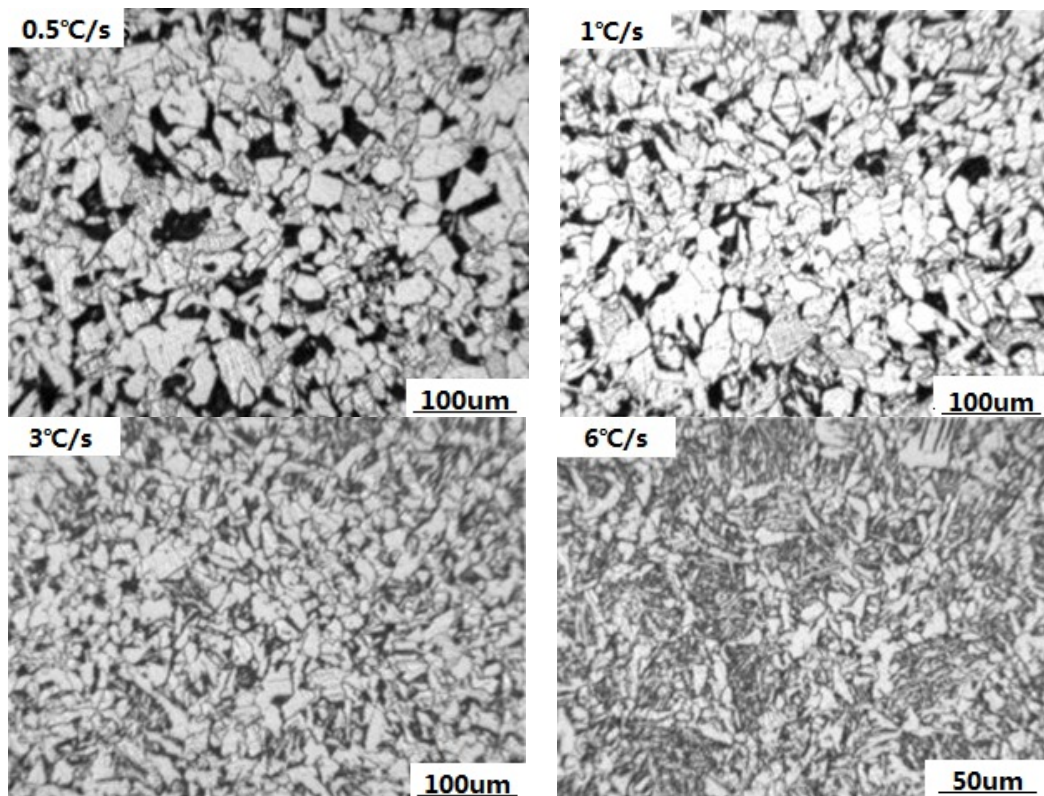
Table 2 The cooling rate and  $t_{8/5}$  corresponding table

cooling/°C/s	0.5	1	3	6	10	15	20	30	40	60
$t_{8/5}/s$	600	300	100	50	30	20	15	10	7.5	5

## 3. RESULTS AND DISCUSSION

### 3.1 Microstructure of V-N-Ti steel experienced by welding thermal simulation

The microstructure of the V-N-Ti steel shown in Figure 2 was obtained from specimens subjected to welding thermal simulation with different cooling rates. According to Figure 2, the microstructure is shown to be varied with different cooling rates. When the cooling rate is less than 3 °C/s, the microstructure is composed of polygonal ferrite and pearlite. Moreover, with the cooling rate increasing, the grain size is fine, as well as, the amount of pearlite decreases; As the cooling rate in the range of 6-10 °C/s, the microstructure mainly consists of proeutectoid ferrite, acicular ferrite and Widmanstatten ferrite that nucleate at the grain boundaries; When the cooling rate was increased up to 20 °C/s, the microstructure is the mixture of acicular ferrite, granular bainite and a little amount of proeutectoid ferrite; The microstructure is mainly composed of bainite, acicular ferrite and a little amount of proeutectoid ferrite and lath bainite at the cooling rate of 40 °C/s; When the cooling rate is 60 °C/s, the microstructure is mainly lath bainite.



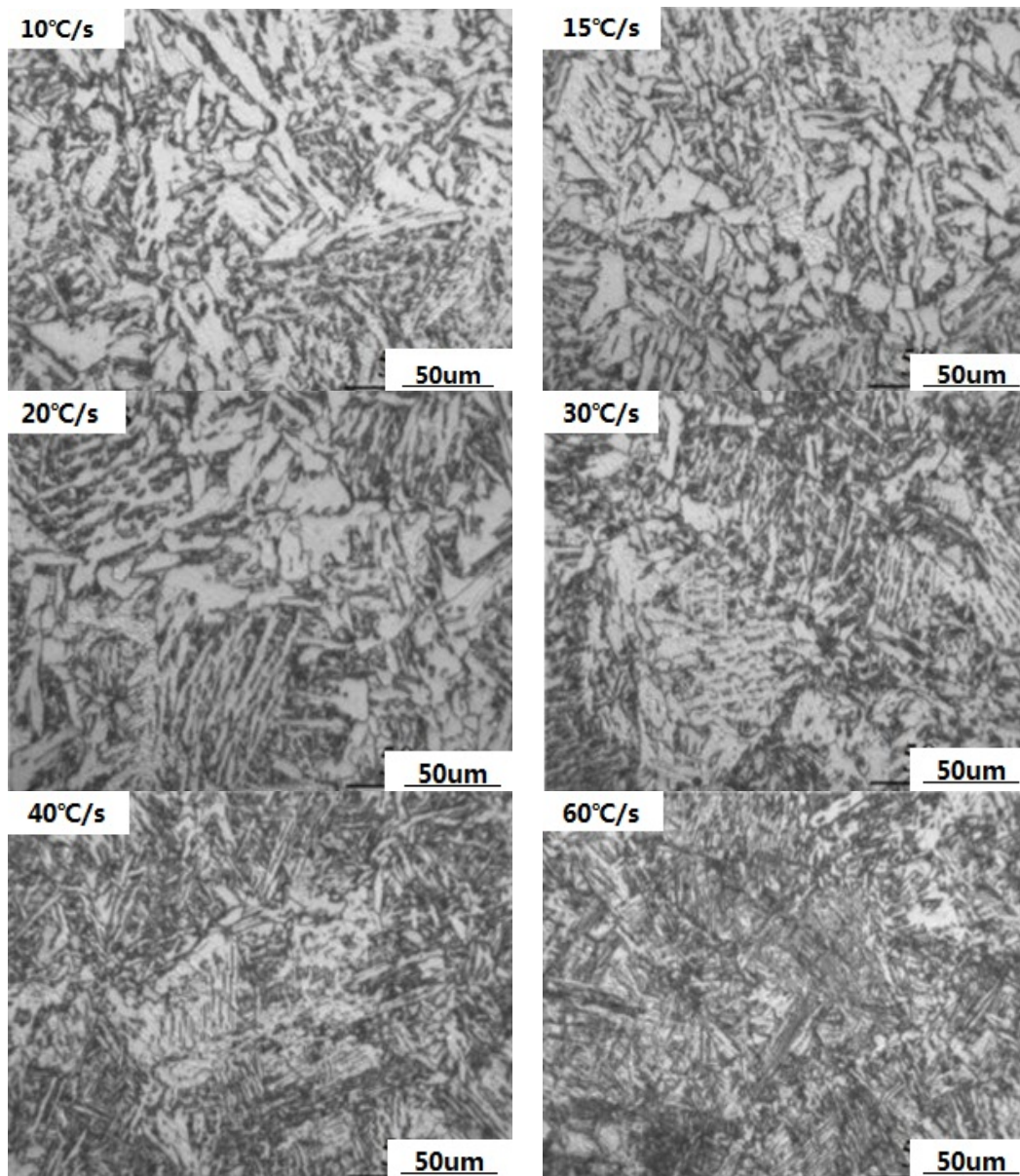
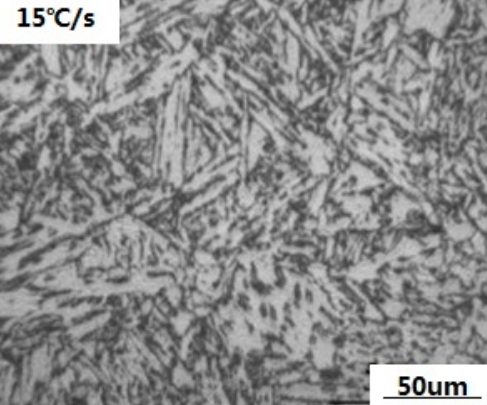
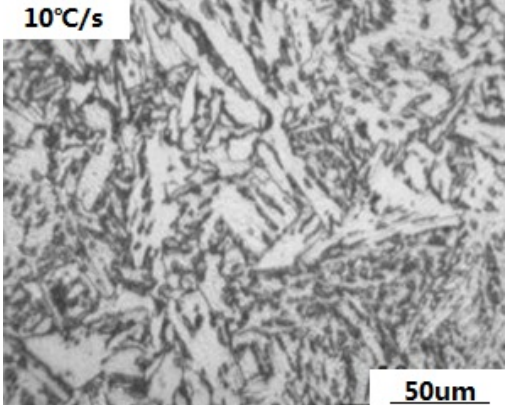
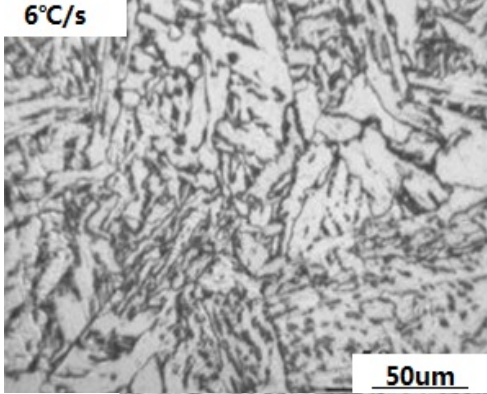
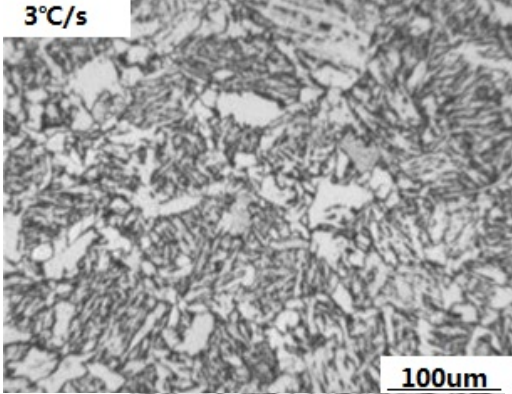
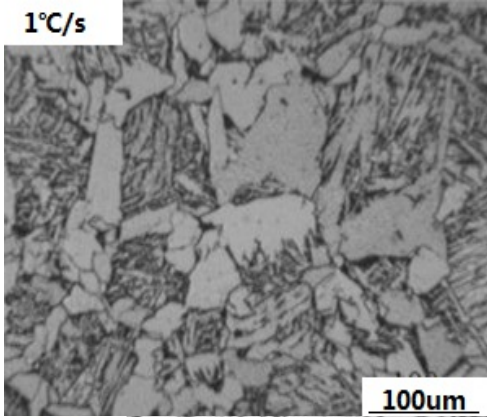
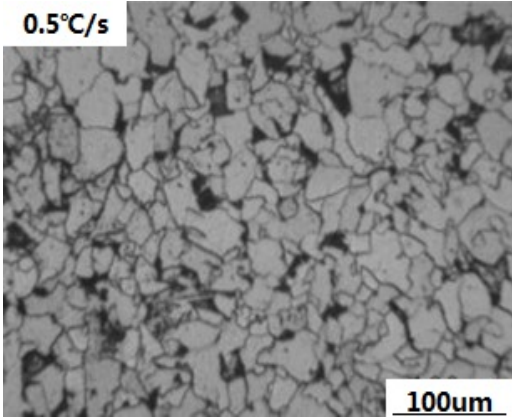


Fig. 2 Microstructure of V-N-Ti steel experienced by welding simulation under different cooling rates

### 3.2 Microstructure of V-Nb-Ti steel experienced by welding thermal simulation

The microstructure of the V-Nb-Ti steel shown in Figure 3 was obtained from specimens subjected to welding thermal simulation with different cooling rates. Based on Figure 3, it can be seen that when the cooling rate is less than 0.5 °C/s, the microstructure is composed of polygonal ferrite and pearlite; with the cooling rate increasing up to 1 °C/s, the original austenitic grain boundaries visualize clearly due to proeutectoid ferrite that nucleates at the grain boundaries. There are much widmanstatten structure throughout the entire original austenitic grain, moreover, a little amount of acicular ferrite appears in the original austenitic grain; with the cooling rate

increasing up to 6 °C/s, a large amount of granular bainite appears. Meanwhile, there is still a little amount of proeutectoid ferrite, which discontinuously distributes at the original austenitic grain boundaries; The microstructure is mainly granular bainite with cooling rates in the range of 10-40 °C/s; When the cooling rate is more than 40 °C/s, the microstructure is composed of granular bainite and lath bainite, and with cooling rate increasing, the amount of lath bainite increases.



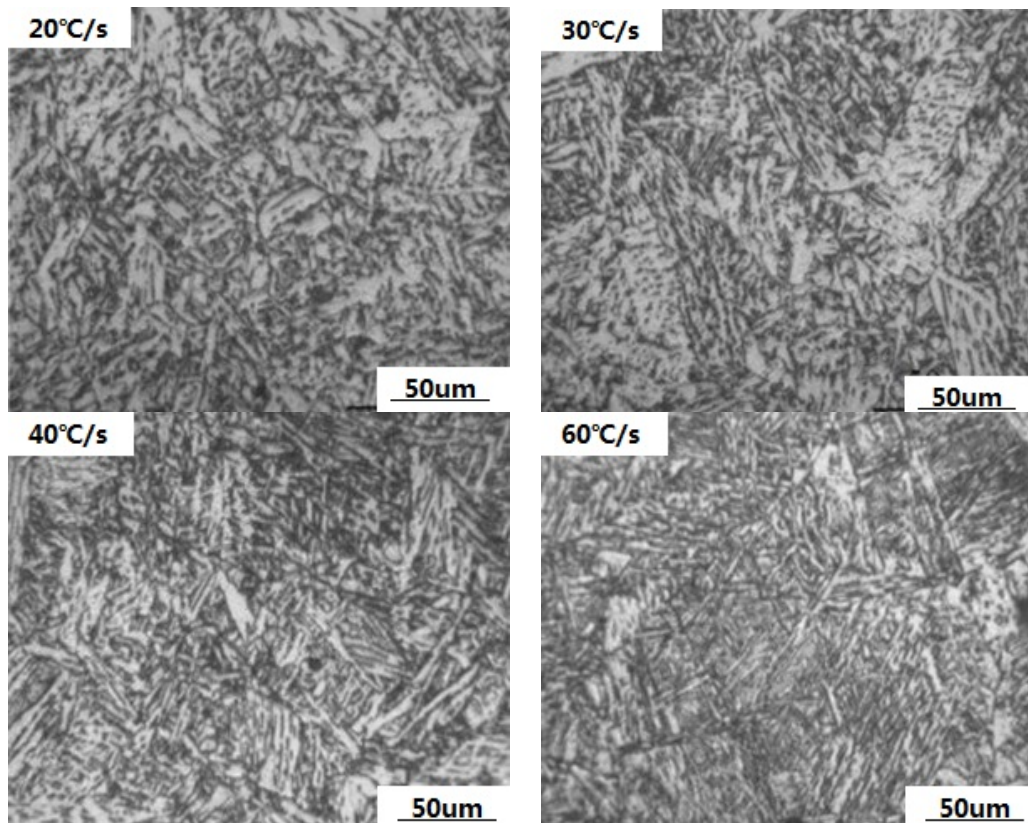


Fig. 3 Microstructure of V-Nb-Ti steel experienced by welding simulation under different cooling rates

### 3.3 SHCCT and HV curve

The experimental data can be dealt with Origin software, and according to the microstructures under different cooling rates, the SHCCT curves of V-N-Ti and V-Nb-Ti steels were obtained.

SHCCT curve of V-N-Ti steel is shown in Figure 4, under the conditions of lower cooling rate (the cooling rate is less than 5 °C/s), the microstructure after transformation is composed of polygonal ferrite and pearlite; when cooling rate is in the range of 6-15 °C/s, the microstructure is composed of polygonal ferrite and acicular ferrite; With the cooling rate increasing, the microstructure consists of acicular ferrite and bainite, and the microstructure is mainly bainite with the cooling rate increasing up to 40 °C/s<sup>[6]</sup>.

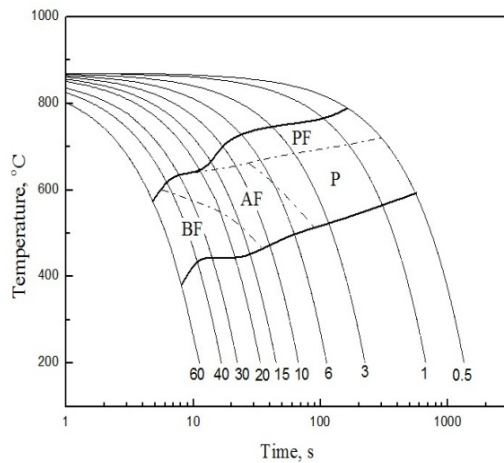


Fig. 4 SHCCT curve of V-N-Ti steel

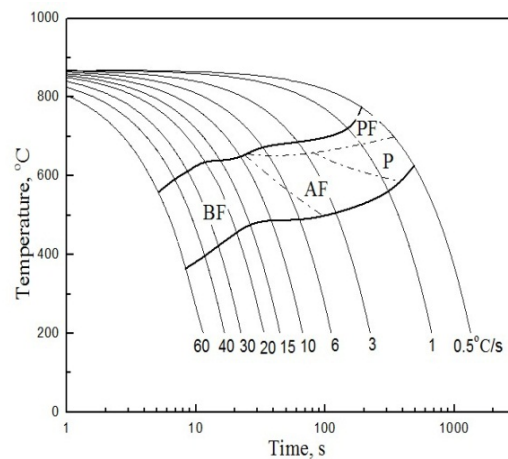


Fig. 5 SHCCT curve of V-Nb-Ti steel

SHCCT curve of V-Nb-Ti steel is shown in Figure 5. From Figure 5, it can be seen that bainite transformation is the primary phase transformation when the cooling rate is more than 10 °C/s; while the cooling rate is less than 6 °C/s, the microstructure after transformation is composed of polygonal ferrite, pearlite and acicular ferrite.

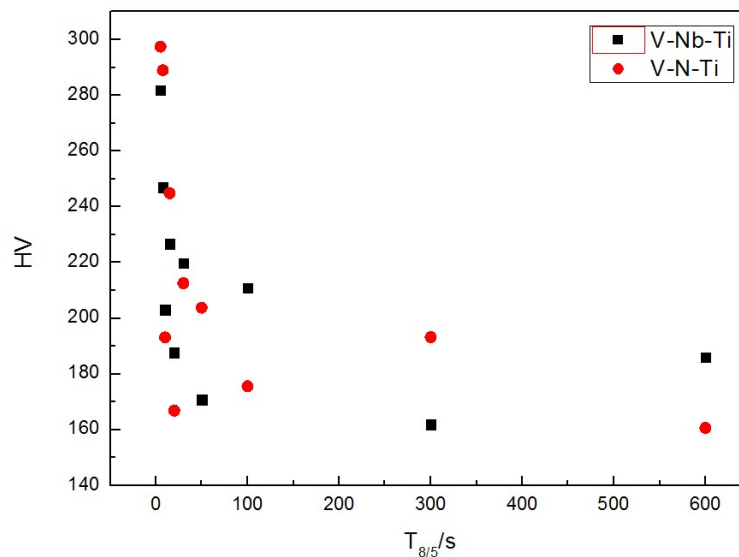


Fig. 6 the relationship between the hardness and  $T_{8/5}$

It can be seen from Figure 6, V-N-Ti steel and V-Nb-Ti steel have high hardness when the  $t_{8/5}$  is short, and hardness of V-N-Ti steel is larger than that of V-Nb-Ti steel. The hardness of V-N-Ti steel reaches the minimum when the  $t_{8/5}$  is 600s. It also can be seen from the value of HV, with the cooling rate increasing, namely, the  $t_{8/5}$  is reducing, hardness of the two steels increased. The value of hardness of bainite and acicular ferrite are almost similar in our test, probably owing to their transition temperatures are close, though their microstructures result from different nucleation ways and have different morphologies. It can be deduced from the analysis of the microstructure and SHCCT that the  $t_{8/5}$  has an important effect on the integrated properties of HAZ. When the appropriate  $t_{8/5}$  is chosen, good welding HAZ microstructures can be obtained.

## 4. CONCLUSIONS

(1) When the cooling rate is lower (less than 5°C/s), the microstructure after transformation is composed of polygonal ferrite and pearlite; When the cooling rate is in the range of 6-15°C/s, the microstructure is mainly composed of polygonal ferrite and acicular ferrite; With the cooling rate increasing, the microstructure consists of acicular ferrite and bainite, and mostly bainite until the cooling rate increased up to 40°C/s.

(2) The bainite transformation mainly occurred when cooling rate is more than 10 °C/s; when cooling rate is less than 6 °C/s, the microstructure after transformation mainly consists of polygonal ferrite, pearlite and acicular ferrite.

(3) The Vickers hardness of HAZ is larger when the  $t_{8/5}$  reducing, the  $t_{8/5}$  has an important effect on the integrated properties of HAZ. When the appropriate  $t_{8/5}$  is chosen, good welding HAZ microstructures can be obtained.

## ACKNOWLEDGMENTS

The authors would like to acknowledge PanGang Group and Vanadium International Technical Committee for their financial supports and FRF-IC-11-005.

## REFERENCES

- [1] Chai Feng, Yang Cai-fu, Zhang Yong-quan. (2005), "Coarse-grain Heat Affected Zone Microstructure and Toughness of Copper-Bearing Age-Hardening Steels", J. Central Iron and Steel Research Institute, Vol.18(2),1-2.
- [2] M.SHOME and O.N.MOHANTY. (2006), "Continuous Cooling Transformation Diagrams Applicable to the Heat-Affected Zone of HSLA-80 and HSLA-100 Steels", J. Metallurgical and Materials Transactions, Vol. 37(7),1-3.
- [3] J.B.Liu, L.J.Hu. (2007). "MICROSTRUCTURE TRANSFORMATION IN THE WELDING HEAT AFFECTED ZONE OF 800MPa GRADE ULTRA FINE STRUCTURED STEEL", J.ACTA METALLURGICA SINICA, Vol.17(3),238-240.
- [4] FANG Fang, YONG Qi-long, YANG Cai-fu. (2009). "Microstructure and Precipitation Behavior in HAZ of V and Ti Microalloyed Steel", J. JOURNAL OF IRON AND STEEL RESEARCH, Vol.16(3),68-69.
- [5] Yaowu Shi, Dong Chen, Yongping Lei. (2004). "HAZ microstructure simulation in welding of a ultrafine grain steel", J. Computational Materials Science, Vol.31(4),379-388.
- [6] BY M. I. ONSØIEN, M. M'HAMDI, AND A. MO. (2009). "A CCT Diagram for an Offshore Pipeline Steel of X70 Type", J. SUPPLEMENT TO THE WELDING JOURNAL, Vol.88(1),1-2.